

Stochastic resonance with different periodic forces in overdamped
two coupled anharmonic oscillators

V.M. Gandhimathi^a, K. Murali^b, S. Rajasekar^{a,*}

^a*School of Physics, Bharathidasan University,
Tiruchirapalli-620 024, Tamilnadu, India*

^b*Department of Chemical Engineering, Anna University,
Chennai-600 025, Tamilnadu, India*

*Corresponding author. E-mail: rajasekar@physics.bdu.ac.in

Abstract

We study the stochastic resonance phenomenon in the overdamped two coupled anharmonic oscillators with Gaussian noise and driven by different external periodic forces. We consider (i) sine, (ii) square, (iii) symmetric saw-tooth, (iv) asymmetric saw-tooth, (v) modulus of sine and (vi) rectified sinusoidal forces. The external periodic forces and Gaussian noise term are added to one of the two state variables of the system. The effect of each force is studied separately. In the absence of noise term, when the amplitude f of the applied periodic force is varied cross-well motion is realized above a critical value (f_c) of f . This is found for all the forces except the modulus of sine and rectified sinusoidal forces. For fixed values of angular frequency ω of the periodic forces, f_c is minimum for square wave and maximum for asymmetric saw-tooth wave. f_c is found to scale as $Ae^{0.75\omega} + B$ where A and B are constants. Stochastic resonance is observed in the presence of noise and periodic forces. The effect of different forces is compared. The stochastic resonance behaviour is quantized using power spectrum, signal-to-noise ratio, mean residence time and distribution of normalized residence times. The logarithmic plot of mean residence time τ_{MR} against $1/(D - D_c)$ where D is the intensity of the noise and D_c is the value of D at which cross-well motion is initiated shows a sharp knee-like structure for all the forces. Signal-to-noise ratio is found to be maximum at the noise intensity $D = D_{max}$ at which mean residence time is half of the period of the driving force for the forces such as sine, square, symmetric saw-tooth and asymmetric saw-tooth waves. With modulus of sine wave and rectified sine wave, the SNR peaks at a value of D for which sum of τ_{MR} in two wells of the potential of the system is half of the period of the driving force. For the chosen values of f and ω , signal-to-noise ratio is found to be maximum for square wave while it is minimum for modulus of sine and

rectified sinusoidal waves. The values of D_c at which cross-well behaviour is initiated and D_{\max} are found to depend on the shape of the periodic forces.

PACS: 02.50.-r; 05.40.-a; 05.45.-a

Keywords: Over damped two coupled anharmonic oscillators; stochastic resonance; periodic forces; power spectrum, mean residence time; signal-to-noise ratio.

1. Introduction

The phenomenon of stochastic resonance has simulated series of theoretical, numerical and experimental works on the dynamics of multi-stable systems subjected to both periodic and noisy driving. In many nonlinear systems, the occurrence of stochastic resonance has been studied with the external periodic force being of the form $f \sin \omega t$ [1-16]. There are few studies with aperiodic forces. For example, enhancement of response of certain nonlinear systems by the added noise with aperiodic forces is observed [17-20]. Jamming (undesirable noise) occurring in an array of FitzHugh-Nagumo oscillators was found to be suppressed via stochastic resonance by the input aperiodic signals such as weak amplitude modulated, frequency modulated and chaotic signals [21]. Stochastic resonance can happen in the absence of periodic excitation [5, 22] and noise [23, 24] also. The former was called spontaneous stochastic resonance and latter as deterministic stochastic resonance.

In recent years, the dynamics of nonlinear systems with different periodic forces has been studied [25-30]. Particularly, the onset of homoclinic chaos in a damped pendulum driven by a periodic string of pulses modulated by Jacobian elliptic function and periodic δ -function is investigated [25]. The existence of a new multiple-period-doubling bifurcation route to chaos and modified bifurcation structures in the Duffing oscillator perturbed by periodic pulses are reported [26]. Anti-control of chaos is accomplished by adding certain periodic forces [27]. A nonlinear feedback controller that generates chaotic behaviour in an oscillator driven by a distorted force has been proposed [28]. Suppression of chaos by δ -pulse in Duffing-van der Pol oscillator [29] and by a variable shape pulse function in a coupled pendulum-harmonic oscillator system [30] is found.

Certain dynamics are studied with forces other than $f \sin \omega t$. It is important to study a particular dynamics with different types of forces and make a comparative study of effects induced by them. This is because different forms of periodic forces can be generated and easily applied to real mechanical systems and electronic circuits. Further, the study of

influence of various forces in nonlinear systems will be helpful to choose a suitable force in creating and controlling nonlinear behaviours.

Motivated by the above, in the present paper, we wish to study stochastic resonance phenomenon with different periodic forces in the overdamped two coupled anharmonic oscillators given by [31]

$$\dot{x} = a_1x - b_1x^3 + \delta xy^2 + F(t) + \eta(t), \quad (1a)$$

$$\dot{y} = a_2y - b_2y^3 + \delta x^2y. \quad (1b)$$

In eqs(1) $F(t)$ and $\eta(t)$ represent the external forcing term and the noise term respectively. In the absence of external periodic force, noise and damping terms the potential of the two coupled anharmonic oscillators is

$$V(x, y) = -\frac{a_1}{2}x^2 + \frac{b_1}{4}x^4 - \frac{a_2}{2}y^2 + \frac{b_2}{4}y^4 - \frac{\delta}{2}x^2y^2. \quad (2)$$

In a very recent work, Baxter et al [32] considered the eqs(1) as a model for competition between two species. They analysed the probability of survival of the species using the path integral method in eqs(1) without $F(t)$ and adding noise to both the state variables x and y . Different types of intermittent-lag synchronization are shown to occur in a parametrically driven two coupled anharmonic oscillators [33].

The organization of the paper is as follows. In section 2, to be self-content we give the mathematical form of the different external forces used in our study. The effect of periodic forces without noise term is discussed in section 3. For fixed values of the parameters, the system is found to exhibit cross-well periodic orbit above a certain critical value (f_c) of the amplitude of the forces. The value of f_c depends on the shape of the forces. f_c is found to increase with increase in the frequency ω of the forces and scales as $Ae^{0.75\omega} + B$. In section 4 we consider the system in the presence of external periodic force and noise. For each force except the modulus of sine and rectified sinusoidal wave stochastic resonance is observed at D_{\max} at which mean residence time is half of the period of the driving force. Stochastic

resonance is characterized using power spectrum, signal-to-noise ratio, mean residence time and distribution of normalized residence time. We compare the effect of various forces on stochastic resonance phenomenon in terms of its characteristic quantities. Section 5 contains summary and conclusion of our present study.

2. Types of periodic forces

The periodic forces of our interest are

1. sine wave
2. square wave
3. symmetric saw-tooth
4. asymmetric saw-tooth
5. modulus of sine wave
6. rectified sine wave

Figure (1) shows the shape of the above forces. Throughout our study, we fix the period T_0 of all the forces as $2\pi/\omega$.

The mathematical representations of the periodic forces are the following:

(1) Sine wave

The sine wave is given by the form

$$F_{\text{si}}(t) = f \sin \omega t, \quad (3)$$

where f is the amplitude of the force and ω is the angular frequency of the force.

(2) Square wave

The mathematical form of square wave is

$$F_{\text{sq}}(t) = \begin{cases} f, & (2n-2)\pi/\omega < t < (2n-1)\pi/\omega \\ -f, & (2n-1)\pi/\omega < t < 2n\pi/\omega, \quad n = 1, 2, \dots \end{cases} \quad (4)$$

For numerical implementation, we rewrite the force (4) as

$$F_{\text{sq}}(t) = \begin{cases} f, & 0 < t < \pi/\omega \\ -f, & \pi/\omega < t < 2\pi/\omega, \end{cases} \quad (5)$$

where t is taken as $\text{mod}(2\pi/\omega)$. That is, $F_{\text{sq}}(t) = F_{\text{sq}}(t + 2\pi/\omega)$. Its Fourier series is

$$F_{\text{sq}}(t) = \frac{4f}{\pi} \sum_{n=1}^{\infty} \frac{\sin(2n-1)\omega t}{(2n-1)}. \quad (6)$$

(3) Symmetric saw-tooth wave

Symmetric saw-tooth wave is mathematically represented as

$$F_{\text{sst}}(t) = \begin{cases} \frac{4ft}{T_0}, & (2n-2)\pi/\omega < t < \left(\frac{4n-3}{2}\right)\pi/\omega \\ -\frac{4ft}{T_0} + 2f, & \left(\frac{4n-3}{2}\right)\pi/\omega < t < \left(\frac{4n-1}{2}\right)\pi/\omega \\ \frac{4ft}{T_0} - 4f, & \left(\frac{4n-1}{2}\right)\pi/\omega < t < 2n\pi/\omega, \quad n = 1, 2, \dots \end{cases} \quad (7)$$

where T_0 is the period of the force. The numerical implementation of the force is given by

$$F_{\text{sst}}(t) = \begin{cases} \frac{4ft}{T_0}, & 0 < t < \pi/2\omega \\ -\frac{4ft}{T_0} + 2f, & \pi/2\omega < t < 3\pi/2\omega \\ \frac{4ft}{T_0} - 4f, & 3\pi/2\omega < t < 2\pi/\omega, \end{cases} \quad (8)$$

where t is taken as $\text{mod}(2\pi/\omega)$. Its Fourier series is

$$F_{\text{sst}}(t) = \frac{8f}{\pi^2} \sum_{n=1}^{\infty} \frac{(-1)^{(n+1)} \sin(2n-1)\omega t}{(2n-1)^2}. \quad (9)$$

(4) Asymmetric saw-tooth wave

The mathematical representation of the wave form shown in fig.1d is

$$F_{\text{ast}}(t) = \begin{cases} \frac{2ft}{T_0}, & (2n-2)\pi/\omega < t < (2n-1)\pi/\omega \\ \frac{2ft}{T_0} - 2f, & (2n-1)\pi/\omega < t < 2n\pi/\omega, \quad n = 1, 2, \dots \end{cases} \quad (10)$$

The force (10) is rewritten as

$$F_{\text{ast}}(t) = \begin{cases} \frac{2ft}{T_0}, & 0 < t < \pi/\omega \\ \frac{2ft}{T_0} - 2f, & \pi/\omega < t < 2\pi/\omega, \end{cases} \quad (11)$$

where t is taken as $\text{mod}(2\pi/\omega)$. The Fourier series of $F_{\text{ast}}(t)$ is given by

$$F_{\text{ast}}(t) = \frac{2f}{\pi} \sum_{n=1}^{\infty} \frac{(-1)^{(n+1)} \sin n\omega t}{n}. \quad (12)$$

(5) Modulus of sine wave

The modulus of sine wave is given as

$$F_{\text{msi}}(t) = f |\sin(\omega t/2)|. \quad (13)$$

Its Fourier series is

$$F_{\text{msi}}(t) = \frac{2f}{\pi} - \frac{4f}{\pi} \sum_{n=1}^{\infty} \frac{\cos n\omega t}{(4n^2 - 1)}. \quad (14)$$

(6) Rectified sine wave

The mathematical representation of rectified sine wave (fig.1f) is

$$F_{\text{rsi}}(t) = \begin{cases} f, & (2n-2)\pi/\omega < t < (2n-1)\pi/\omega \\ 0, & (2n-1)\pi/\omega < t < 2n\pi/\omega, \quad n = 1, 2, \dots \end{cases} \quad (15)$$

The numerical implementation of the force (15) is

$$F_{\text{rsi}}(t) = \begin{cases} f, & 0 < t < \pi/\omega \\ 0, & \pi/\omega < t < 2\pi/\omega. \end{cases} \quad (16)$$

The Fourier series of rectified sine wave is

$$F_{\text{rsi}}(t) = \frac{1}{\pi} - \frac{2}{\pi} \sum_{n=1}^{\infty} \frac{\cos 2n\omega t}{(4n^2 - 1)} + \frac{\sin \omega t}{2}. \quad (17)$$

for $0 < t < \pi/\omega$ and 0 for $\pi/\omega < t < 2\pi/\omega$.

3. Cross-well motion due to different periodic forces without noise term

In this section we considered the system (1) in the absence of noise term $\eta(t)$ but with different external forces. The parameters of the system are fixed at $a_1 = 1.0$, $a_2 = 1.1$, $b_1 = 1.0$, $b_2 = 1.0$. For this choice, the potential is a four-well potential. The potential wells are designated as V_{++} for $x > 0$, $y > 0$; V_{+-} for $x > 0$, $y < 0$; V_{-+} for $x < 0$, $y > 0$; V_{--} for $x < 0$, $y < 0$. The period of the all the forces is set to $2\pi/\omega$. For each force the response of the system is studied by varying the amplitude of it.

First, we consider the effect of the sinusoidal force $f \sin \omega t$. For a fixed value of ω and for small values of f , four period- T_0 ($2\pi/\omega$) orbits one in each potential well exist. The size of the orbit increases with increase in the value of f . At a critical value of f , f_c , the trajectory makes a cross-well motion forming a coupled orbit. However, the period of the cross-well orbit remains as T_0 . Since the external forcing is added only to x -component of the system, the coupled orbit traverse the wells V_{++} and V_{-+} or the wells V_{+-} and V_{--} depending upon the initial conditions. For f in the range $[0, 50]$, chaotic behaviour is not observed. This is confirmed from the bifurcation diagram and Lyapunov exponent calculations. Similar behaviour is observed for various values of ω in the interval $[0, 1]$ with step size $\omega = 0.05$ and also for other forces except for modulus of sine wave and rectified sine wave. In the case of modulus of sine wave added to x -component of the system the wells V_{-+} and V_{--} alone are oscillating. The wells V_{++} and V_{+-} are stationary. For initial conditions in the well V_{+-} or V_{--} , after the transient evolution the system remains in the well V_{+-} . In the case of rectified sine wave during the first half of the period of the drive cycle only the wells V_{-+} and V_{--} oscillate. Therefore, cross-well behaviour is not observed for f in the range $[0, 50]$ in both the cases.

For the force $f \sin \omega t$ with $\omega = 0.05$, the critical value of f (at which cross-well motion is initiated) is numerically found to be 0.409. For forces such as square, symmetric saw-tooth and asymmetric saw-tooth waves f_c is 0.393, 0.4408 and 0.475 respectively. Figure 2 shows the variation of f_c with ω . In this figure the dots represent numerical result and the continuous lines are the best curve fit. We find that f_c increases with increase in ω . For a fixed ω the f_c for square wave is minimum while it is maximum for asymmetric saw-tooth wave. That is, cross-well motion is initiated at a lower value of f for square wave when compared with other forces. The cross-well motion occurs relatively at a higher value of f in the case of sine, symmetric saw-tooth and asymmetric saw-tooth waves. For all the forces f_c is found to vary with ω as $Ae^{0.75\omega} + B$. The values of (A, B) obtained for square, sine, symmetric saw-tooth and asymmetric saw-tooth forces are $(0.471, -0.130)$, $(0.754, -0.409)$,

(0.987, -0.602) and (1.284, -0.834) respectively.

4. Stochastic resonance with different periodic forces

In the previous section, we studied the effect of different periodic forces separately in the absence of noise term $\eta(t)$. Now, we include the noise term and study the stochastic resonance phenomenon by varying the noise intensity D . Here again we perform the analysis for each force separately. The noise term is chosen as Gaussian random numbers. The parameters are fixed at $a_1 = 1.0$, $a_2 = 1.1$, $b_1 = 1.0$, $b_2 = 1.0$, $\delta = 0.01$ and $\omega = 0.05$. In the absence of noise, the critical value of f at which cross-well orbit occurs for square, sine, symmetric saw-tooth and asymmetric saw-tooth waves are 0.393, 0.409, 0.4408 and 0.475 respectively. The value of f is fixed below f_c . We fix $f = 0.38$ for all the forces so that in the absence of noise the motion is confined to single well alone, that is, there is no cross-well motion. We integrated eqs(1) using a fourth-order Runge-Kutta method with step size $\Delta t = (2\pi/\omega)/N$, $N = 2001$. Noise is added to the state variable x as $x_{i+1} \rightarrow x_{i+1} + \sqrt{\Delta t} D \zeta(t)$ after each integration step Δt . Here $\zeta(t)$ represents Gaussian random numbers with zero mean and unit variance and D denotes noise intensity.

4.1. Cross-well motion and mean residence time

First, we illustrate the effect of noise in the presence of square wave. Cross-well motion is not realized for $D < D_c \approx 0.0002$. At $D = D_c$, orbit switching from one-well to another well is initiated. For example, cross-well behaviour is observed between the two wells V_{++} and V_{-+} at $D = D_c$. Similar behaviour is observed when the square wave is replaced by other wave forms with same ω and f values. However, the value of D_c is found to be different for other forces. D_c values for square, sine, symmetric saw-tooth, asymmetric saw-tooth, modulus of sine and rectified sine waves are 0.0002, 0.0005, 0.002, 0.0025, 0.05 and 0.03 respectively. D_c is relatively low for the square wave.

For each periodic force, the switching between the wells become very rare for D values

just above D_c . However, as D increases switching also increases. To characterize this behaviour we numerically calculated the mean residence time. Residence time τ_R is defined as the duration of the trajectory of the system residing in a well (for example, V_{++}) before jumping to another well (say, V_{-+}) and vice-versa. Mean residence time τ_{MR} in the wells V_{-+} and V_{++} are computed for a set of 10^5 residence times. Rapid variation of τ_{MR} is found when the noise intensity D is varied from D_c . Figure 3a shows $\ln(\tau_{MR})$ versus $1/(D - D_c)$ when the applied force is square wave. Later, we will show that signal-to-noise ratio (SNR) is maximum at this value of D . Different form of variation of τ_{MR} is found for $D < D_{max}$ and $D > D_{max}$. The curve in the fig.3a has a sharp knee at $D = D_{max}$. At this value of D the derivative of τ_{MR} is discontinuous. Sharp-knee shape like variation of maximal Lyapunov exponent versus control parameter is observed for band-merging crisis [34]. Mean residence time τ_{MR} for the other periodic forces are also calculated. The logarithmic plot of τ_{MR} versus $1/(D - D_c)$ is shown in figs.3b-d for sine, symmetric saw-tooth and asymmetric saw-tooth forces. All the plots resemble the knee-like structure. The values of D_{max} are found to be 0.14, 0.1, 0.12 and 0.17 for square, sine, symmetric saw-tooth and asymmetric saw-tooth forces. The maximum SNR values are obtained at these values of D for the above forces.

For the forces depicted in figs.1a-d the sign of the forces is positive during one half of the cycle and negative during the second half of the cycle. For the forces in fig.1e and 1f the sign of the force is never negative. This difference in the forces and the symmetry between the wells have influence on the mean residence time. For the forces shown in figs.1a-d for D values just above D_{max} the τ_{MR} in the wells V_{-+} and V_{++} are same and greater than the period $T_0 = 2\pi/\omega \approx 125.67$ of the drive cycle. As D increases τ_{MR} decreases. In the case of modulus of sine and rectified sine waves, the mean residence time τ_{MR} in the well V_{-+} for D just above D_c is less than $T_0/2 = \pi/\omega \approx 62.83$ while it is greater than T_0 for the other well V_{++} . That is, τ_{MR} is not same for the two wells V_{-+} and V_{++} . τ_{MR} in both the wells decreases with further increase in D . Figures 4 and 5 show the variation of τ_{MR} with D for

the modulus of sine and rectified sine waves respectively.

4.2. Stochastic resonance

Time series plot in the presence of external square wave for few values of noise intensity D is shown in fig.6. For small values of D the system exhibit the same periodic behaviour of noise free case but slightly perturbed by the noise. For $D < D_c = 0.0002$, the trajectory of the system resides in a single well as in fig.6a. At the critical value D_c the trajectory jumps randomly from one well to another. In fig.6b for $D = 0.001$ just above D_c the state variable x switches irregularly and rarely between the wells V_{++} and V_{-+} . In the presence of forcing, the system initially in the well, say, V_{++} is forced by the noise to leave the well. Then the system enters the well V_{-+} and wanders irregularly there for some time and jumps back to the well V_{++} and so on. For $D = 0.001$ τ_{MR} is computed as ≈ 790 . The switching is not periodic. The residence times are randomly distributed. τ_{MR} decreases with increase in D . For $D = 0.14$, τ_{MR} is found to be $\approx \pi/\omega \approx 62.83$. In this case nearly periodic switching between the wells V_{++} and V_{-+} occur. There is a co-operation between the periodic driving force and the noise. The x -component of the trajectory switches between the positive and negative values with the period approximately half of the period of the applied external periodic force. This is clearly seen in fig.6c.

For large values of D , the motion is dominated by the noise term. Figure 6d shows the trajectory for $D = 2.5$ where the trajectory jumps erratically between the wells. That is, loss of coherence is produced by the large noise intensity. For D in the range $[D_c, 4]$, jumping motion between the wells V_{++} and V_{-+} alone observed. The system (1) is studied with different periodic forces as a function of noise intensity. We observed similar response of the system for all the forces except modulus of sine and rectified sine waves.

The trajectory of the system exhibited periodic transitions between the wells at $D_{\max} = 0.1, 0.12, 0.17$ for sine, symmetric saw-tooth and asymmetric saw-tooth waves. Synchronization of the input wave form with the output at these values of D is shown in fig.7 for

various forces. In this figure for all the forces at $D = D_{\max}$ we can notice a common feature. Nearly at the end of one half of a drive cycle the trajectory in one well is likely to jump to the another well and after the next half cycle it is likely to return back. This is the signature of stochastic resonance.

4.3. Characterization of stochastic resonance by signal-to-noise ratio

We characterize the stochastic resonance phenomenon in terms of SNR and the peak value at the half driving frequency in the distribution of normalized residence times. SNR is calculated from the power spectrum of the state variable x . To compute power spectrum, we have used fast Fourier transform technique [35, 36]. The power spectrum is obtained using a set of 2^{10} data collected at a time interval of $(2\pi/\omega)/10$. To get more accurate power spectrum we computed it for 25 different realization of Gaussian random numbers and then obtained the average spectrum.

In the absence of noise term, the power spectrum of x component of the system with different periodic forces is first analyzed. With square wave as the external forcing, the power spectrum has peaks at few odd and even integral multiples of the forcing frequency. When the noise is included, the peaks at odd integral multiples are alone dominant. With increase in noise intensity D , the height of the peaks increase up to $D = D_{\max}$ (at which $\tau_{MR} \approx \pi/\omega$) and then decrease. The power spectrum for four values of D in the presence of square wave is shown in fig.8. Dominant peaks are seen at $\Omega = 0.05$ and 0.15 .

Signal-to-noise ratio is calculated from power spectrum using the formula

$$SNR = 10 \log_{10}(S/N) \text{ dB.} \tag{18}$$

In eq(18) S and N are the amplitudes of the signal peak and the noise background respectively. S is read directly from the power spectrum at the frequency ω of the driving periodic force. To calculate the background of the power spectrum about ω we considered the power spectrum in the interval $\Omega = \omega - \Delta\omega$ and $\omega + \Delta\omega$ after subtracting the point namely $\Omega = \omega$

representing the stochastic resonance spike. The average value of the power spectrum in the above interval is taken as background noise level at ω . We have chosen $\Delta\omega = 0.01$. Figure 9a shows the plot of SNR as a function of D for square wave. The calculated SNR increases rapidly with the noise intensity D , peaks at the critical value $D_{\max} = 0.14$ and then decreases slowly for $D > D_{\max}$. With modulus of sine and rectified sine waves for small values of noise intensity D , rare switching between the wells V_{++} and V_{-+} is observed. However, periodic switching with the half of the period of the drive cycle is not observed when D is varied. Figure 9b shows SNR versus D for various applied forces. With the forces such as sine, square, symmetric saw-tooth and asymmetric saw-tooth waves, SNR has a peak at $D = D_{\max}$ at which $\tau_{MR} \approx \pi/\omega$ and there is almost a periodic switching between the wells V_{-+} and V_{++} as shown in fig.7. For the forces given in figs.1e-f the τ_{MR} in V_{-+} is always less than π/ω . However, stochastic resonance is observed at the value of D at which the sum of the mean residence times of both the wells V_{-+} and V_{++} is $\approx \pi/\omega$. This happens at $D = 0.35$ and $D = 0.3$ for modulus of sine and rectified sine waves respectively. For these forces SNR initially decreases with increase in D from D_c for a while, increases with increase in D , reaches a maximum value and then decreases with further increase in D . SNR is found to be highest for square wave. Modulus of sine wave and rectified sine wave yields the minimum SNR value.

4.4. Characterization of stochastic resonance by probability distribution of normalized residence times

The probability distribution of normalized residence times denoted as P can also be used to quantify stochastic resonance. Normalized residence time is calculated as follows. For a fixed noise intensity D the residence time τ_R in a well is computed for a set of 10^5 transitions. Then, normalized residence times are obtained by dividing τ_R by the period T_0 of the applied force. Then we calculated $P(\tau_R/T_0)$. P is found to be same for the wells V_{-+} and V_{-+} . In fig.10 we have plotted P versus τ_R/T_0 for four values of noise intensity with the applied periodic force being square wave. We observe a series of Gaussian like peaks, centered at

odd integral multiples of $T_0/2$. The heights of these peaks decrease exponentially with their order n . The strength P_1 of the peak at $\tau_R = T_0/2$ is a measure of the synchronization between the periodic forcing and the switching between the wells. The variation of P_1 can be used to characterize the stochastic resonance phenomenon. For values of D nearly above D_c , τ_R/T_0 is distributed relatively over wide interval of time (fig.10a). As D increases the range of τ_R decreases and P of smaller τ_R increases. At $D = D_{\max}$ as shown in fig.10c the noise induced oscillations have period $\approx T_0/2$ and hence $P(\tau_R/T_0 = 1/2)$ becomes maximum. As D is further increased P_1 decreases. Similar behaviour is observed for the periodic forces given in figs.1a-d. Figure 11 shows P_1 versus D for various forces. The effect of various forces on P_1 can be clearly seen in this figure. For small values of D , τ_R/T_0 is distributed over wide interval of time. Therefore, P_1 increases with increase in D , reaches a maximum at $D = D_{\max}$ and then decreases. With the modulus of sine and rectified sine waves, the peak P_1 at $\tau_R/T_0 = 1/2$ is numerically calculated for various values of D in the wells V_{-+} and V_{++} . For the well V_{-+} , the value of P_1 decreases with increase in the value of D . But for the well V_{++} , P_1 increases with increase in D reaches a maximum at which SNR is maximum and then decreases. Figures 12 and 13 show the plot of P_1 versus noise intensity D for the forces in fig.1e and fig.1f respectively.

5. Summary and conclusion

We have studied numerically the effect of different periodic forces and Gaussian noise in the overdamped two coupled anharmonic oscillators eqs(1). In order to compare the effect of external forces we have fixed the period of the forces as $2\pi/\omega$. The average of all the forces over one drive cycle is zero except for modulus of sine wave and rectified sine wave. The system shows periodic behaviour in the presence of external periodic forces and in the absence of noise term. Since the forcing is added only to x -component, the system performs transitions between the wells V_{++} and V_{-+} only. The value of f_c is found to be small for square wave when compared with other forces. Cross-well behaviour is delayed in the case of sine, symmetric saw-tooth and asymmetric saw-tooth forces. With the other two forces,

cross-well motion is not observed. Stochastic resonance is observed with all the forces used. The mean residence time, power spectrum, SNR and distribution of normalized residence times are used to characterize stochastic resonance. The features of stochastic resonance are found to be same for the forces such as sine, square, symmetric saw-tooth and asymmetric saw-tooth waves. Maximum SNR is obtained at the value of D at which sum of the residence times $\approx \pi/\omega$ for modulus of sine and rectified sine waves respectively. The values of D_c and D_{max} are found to be different for different periodic forces. Signal-to-noise ratio values are found to depend on the type of forcing used. Square wave gives maximum SNR . Modulus of sine wave and rectified sine wave yields minimum SNR . The height of the peak P_1 at D_{max} obtained from normalized residence time distribution vary with the periodic forces. In the nonlinear dynamics literature, many interesting results have been obtained with the quasiperiodic, chaotic, aperiodic forces and with the different noise terms. Therefore, it is interesting to study the stochastic resonance behaviour with the above forces.

Acknowledgement

The work reported here forms part of a Department of Science and Technology, Government of India research project. We are thankful to Dr.K.P.N. Murthy for stimulating discussion.

REFERENCES

- [1] B. Mc Namara, K. Wiesenfeld, Theory of stochastic resonance. *Phys. Rev. A* 1989; 39: 4854-4869.
- [2] F. Moss, Stochastic resonance. *Ber. Bunsenges. Phys. Chem.* 1991; 95: 303-311.
- [3] A. Neiman, L. Schimansky-Geier, Stochastic resonance in two coupled bistable systems. *Phys. Lett. A* 1995; 197: 379-386.
- [4] X. Godivier, F.C. Blondeau, Stochastic resonance in the information capacity of a non-linear dynamical system. *Int. J. Bifurcation and Chaos* 1998; 8: 581-589.
- [5] F. Marchesoni, L. Gammaitoni, F. Apostolico, S. Santucci, Numerical verification of bonafide stochastic resonance. *Phys. Rev. E* 2000; 62: 146-149.
- [6] R. Chacon, Resonance phenomena in bistable systems. *Int. J. Bifurcation and Chaos* 2003; 13: 1823-1829.
- [7] M.F. Carusela, J. Codnia, L. Romanelli, Stochastic resonance: Numerical and experimental devices. *Physica A* 2003; 330: 415-420.
- [8] Xue-Juan Chang, Limit cycles and stochastic resonance in a periodically driven Langevin equation subjected to white noise. *J. Phys. A: Math. Gen.* 2004; 37: 7473-7484.
- [9] D. Valenti, A. Fiasconaro, B. Spagnolo, Stochastic resonance and noise delayed extinction in a model of two competing species. *Physica A* 2004; 331: 477-486.
- [10] R. Benzi, A. Sutera, Stochastic resonance in two-dimensional Landau-Ginzburg equation. *J. Phys. A: Math. Gen.* 2004; 37: L391-L398.
- [11] L. Gammaitoni, P. Hanggi, P. Jung, K. Marchesoni, Stochastic resonance. *Rev. Mod. Phys.* 1998; 70: 223-287.
- [12] P. Jung, Periodically driven stochastic systems. *Phys. Rep.* 1993; 234: 175-295.

- [13] K. Wiesenfeld, F. Jaramillo, Minireview of stochastic resonance. *Chaos* 1998; 8: 539-548.
- [14] V.S. Anishchenko, A.B. Neiman, F. Moss, L. Schimansky-Geier, Stochastic resonance: Noise-enhanced order. *Phys. Usp.* 1999; 42: 7-36.
- [15] P. Hanggi, Stochastic resonance in biology. *Chem. Phys. Chem.* 2002; 3: 285-290.
- [16] G. Ambika, K. Menon, K.P. Harikrishnan, Aspects of stochastic resonance in Josephson junction, bimodal map and coupled map lattice. *Pramana J. Physics* 2005; 64: 535-542.
- [17] J.J. Collins, C.C. Chow, A.C. Capela, T.T. Imhoff, Aperiodic stochastic resonance. *Phys. Rev. E* 1996; 54: 5575-5584.
- [18] C. Heneghan, C.C. Chow, J.J. Collins, T.T. Imhoff, S.M. Lowen, M.C. Teich, Information measures quantifying aperiodic stochastic resonance. *Phys. Rev. E* 1996; 54: R2228-R2231.
- [19] J.J. Collins, T.T. Imhoff, P. Grigg, Noise-enhanced information transmission in rat SA1 cutaneous mechanoreceptors via aperiodic stochastic resonance. *Journal of Neurophysiology.* 1996; 76: 642-645.
- [20] A. Capurro, K. Pakdaman, T. Nomura, S. Sato, Aperiodic stochastic resonance with correlated noise. *Phys. Rev. E* 1998; 58: 4820-4827.
- [21] Y.C. Lai, Z. Liu, A. Nachman, L. Zhu, Suppression of jamming in excitable systems by aperiodic stochastic resonance. *Int. J. Bifurcation and Chaos* 2004; 14: 3519-3539.
- [22] M. Qian, X. Zhang, Stochastic resonance via switching between the two stable limit cycles on a cylinder. *Phys. Rev. E* 2002; 65: 011101-011104.
- [23] S. Sinha, Noise-free stochastic resonance in simple chaotic systems. *Physica A* 1999; 270: 204-214.
- [24] K. Arai, K. Yohima, S. Mituzani, Dynamical origin of deterministic stochastic resonance. *Phys. Rev. E* 2001; 65: 015202-1-015202-4.

- [25] R. Chacon, Chaos and geometrical resonance in the damped pendulum subjected to periodic pulses. *J. Math. Phys.* 1997; 38: 1477-1483.
- [26] A. Venkatesan, S. Parthasarathy, M. Lakshmanan, Occurrence of multiple period-doubling bifurcation route to chaos in periodically pulsed chaotic dynamical systems. *Chaos, Solitons and Fractals* 2003; 18: 891-898.
- [27] Z.M. Ge, W.Y. Leu, Anti-control of chaos of two-degrees freedom loudspeaker system and chaos synchronization of different order systems. *Chaos, Solitons and Fractals* 2004; 20: 503-521.
- [28] K. Konishi, Generating chaotic behaviour in an oscillator driven by periodic forces. *Phys. Lett. A* 2003; 320: 200-206.
- [29] A.Y.T. Leung, L. Zengrong, Suppressing chaos for some nonlinear oscillators. *Int. J. Bifurcation and Chaos* 2004; 14: 1455-1465.
- [30] R. Chacon, Inhibition of chaos in Hamiltonian systems by periodic pulse. *Phys. Rev. E* 1994; 50: 750-753.
- [31] V.M. Gandhimathi, K. Murali, S. Rajasekar, Stochastic resonance in overdamped two coupled anharmonic oscillators. *Physica A* 2005; 347: 99-116.
- [32] G. Baxter, A.J. McKane, Quantifying stochastic outcomes. *Phys. Rev. E* 2005; 71: 011106-1-011106-15.
- [33] A.N. Pisarchik, R. Jaimes-Rategui, Intermittent lag synchronization in a driven system of coupled oscillators. *Pramana J. Physics* 2005; 64: 503-511.
- [34] V. Mehra, R. Ramaswamy, Maximal Lyapunov exponent at crises. *Phys. Rev. E* 1996; 53: 3420-3424.
- [35] W.H. Press, S.A. Teukolsky, W.T. Wellerling, B.P. Flannery, *Numerical Recipes in Fortran*, Cambridge University Press, Cambridge, 1993.

[36] Tao Pang, *An introduction to computational physics*, Cambridge University Press, Cambridge, 1997.

FIGURES

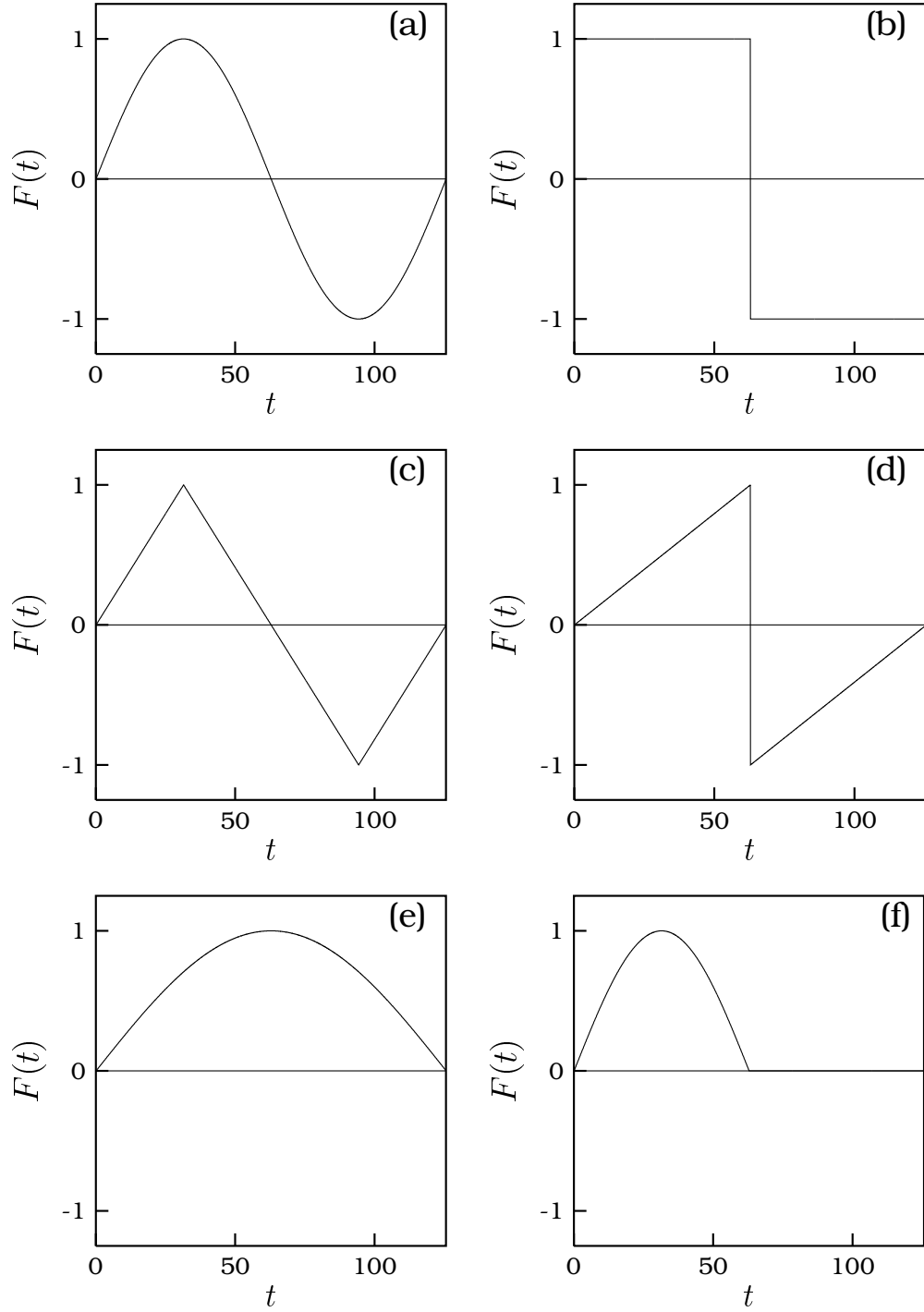


FIG. 1. Form of different periodic forces: (a) sine wave, (b) square wave, (c) symmetric saw-tooth wave, (d) asymmetric saw-tooth wave, (e) modulus of sine wave and (f) rectified sine wave. For all the forces the period T_0 is $2\pi/\omega$ with $\omega = 0.05$ and the amplitude is set to 1.

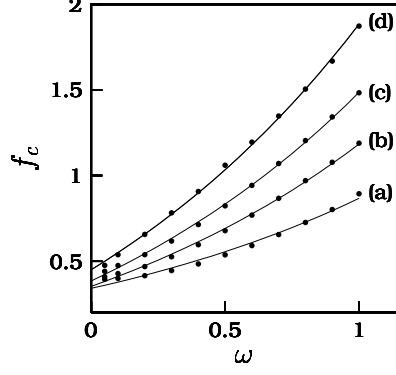


FIG. 2. f_c versus ω for various forces. The curves (a), (b), (c) and (d) are for the square wave, sine wave, symmetric saw-tooth wave and asymmetric saw-tooth wave respectively. Dots represent numerical data and continuous lines are the best curve fits.

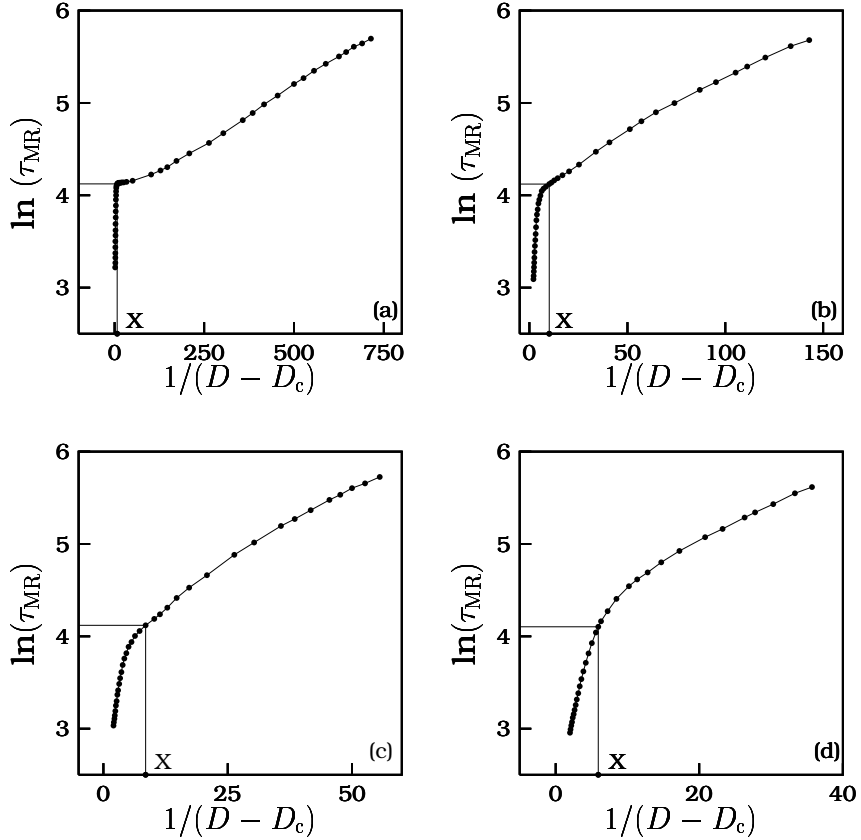


FIG. 3. Mean residence time in logarithmic scale versus $1/(D - D_c)$ for (a) square wave, (b) sine wave, (c) symmetric saw-tooth wave and (d) asymmetric saw-tooth wave. The parameters of the system are $a_1 = 1.0$, $a_2 = 1.1$, $b_1 = 1.0$, $b_2 = 1.0$, $\delta = 0.01$, $f = 0.38$ and $\omega = 0.05$. The symbol X indicates the value of $1/(D_{\max} - D_c)$ where D_{\max} is the value of D at which $\tau_{MR} = \pi/\omega$.

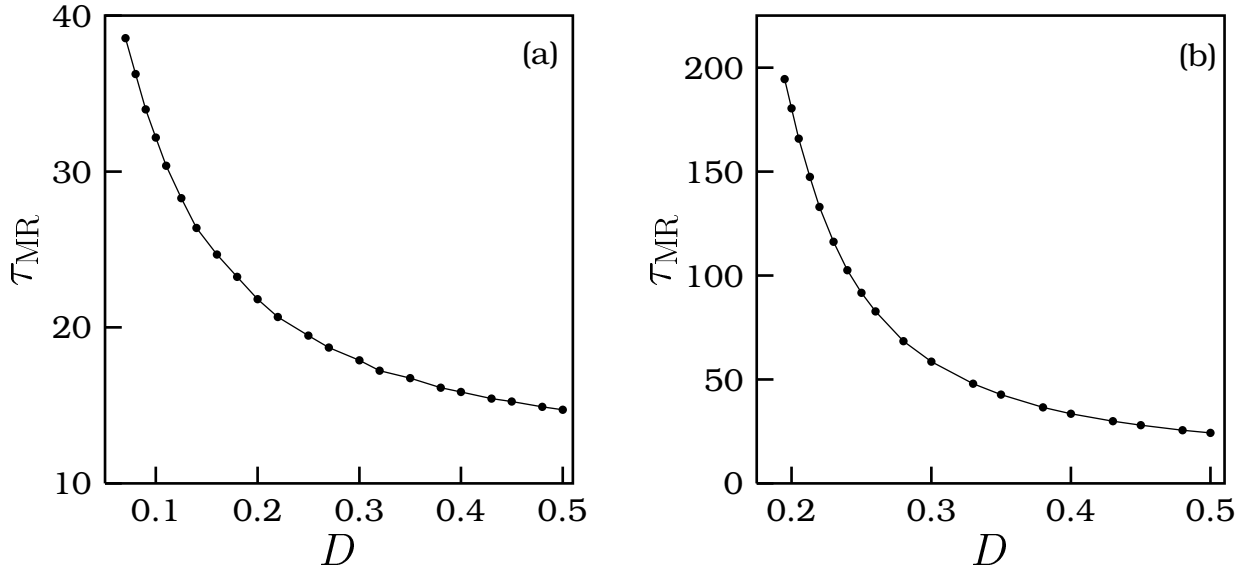


FIG. 4. Mean residence time in the wells (a) V_{-+} and (b) V_{++} for the force modulus of sine wave. In the subplot (b) for clarity τ_{MR} is plotted from $D = 0.2$.

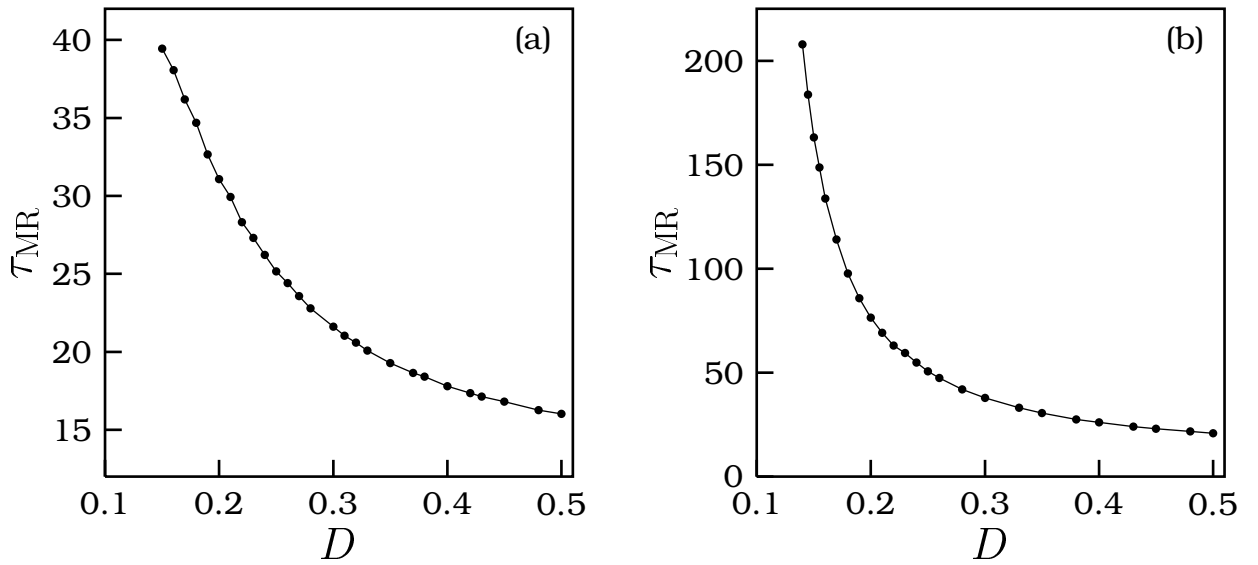


FIG. 5. Mean residence time of system (1) in the wells (a) V_{-+} and (b) V_{++} for the rectified sine wave.

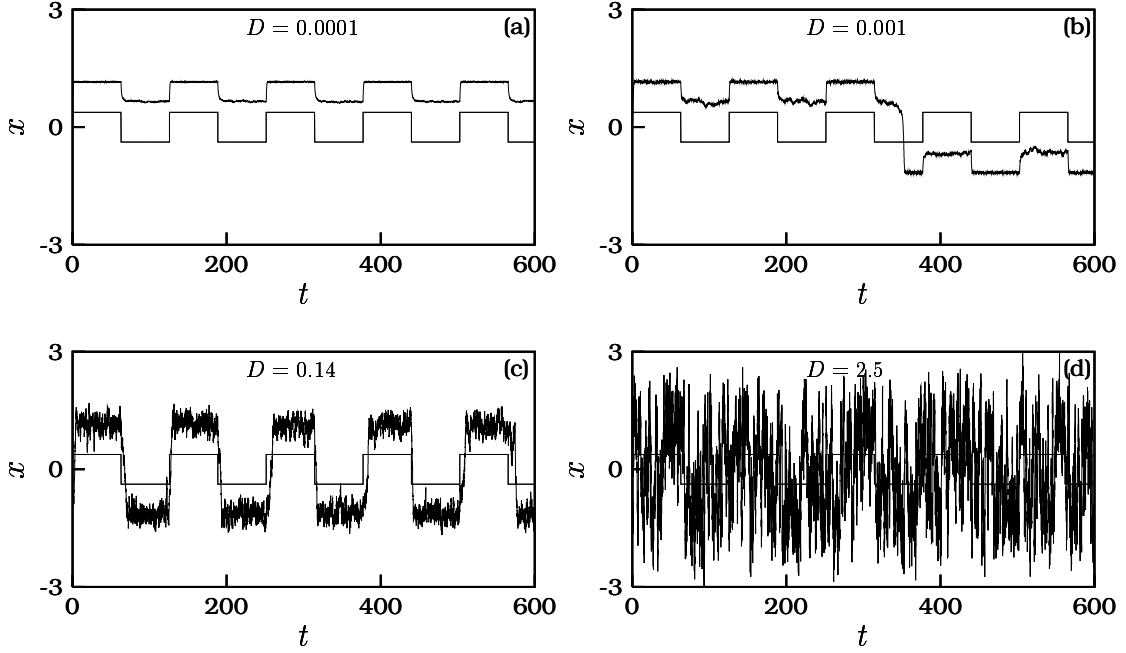


FIG. 6. Time series plot of eqs(1) in the presence of square wave for few values of noise intensity D . The parameters of the system are $a_1 = 1.0$, $a_2 = 1.1$, $b_1 = 1.0$, $b_2 = 1.0$, $\delta = 0.01$, $f = 0.38$ and $\omega = 0.05$. The applied square wave is also plotted.

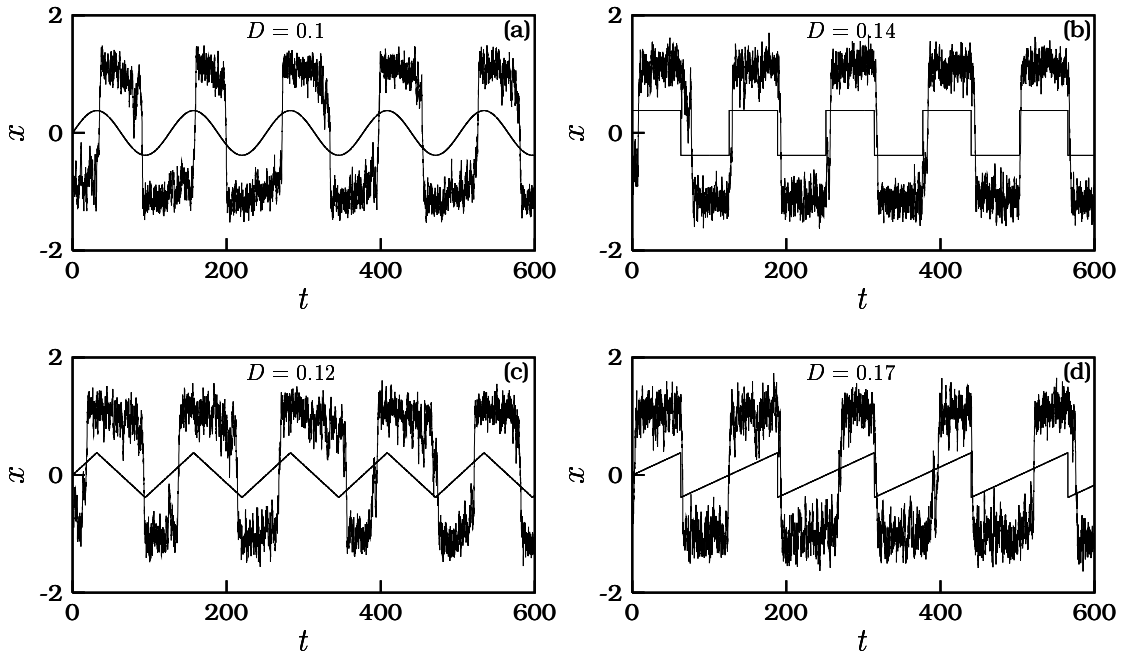


FIG. 7. Synchronization of the output signal with the different applied periodic forces such as (a) sine wave, (b) square wave, (c) symmetric saw-tooth wave and (d) asymmetric saw-tooth wave. In all the subplots the value of D is D_{\max} .

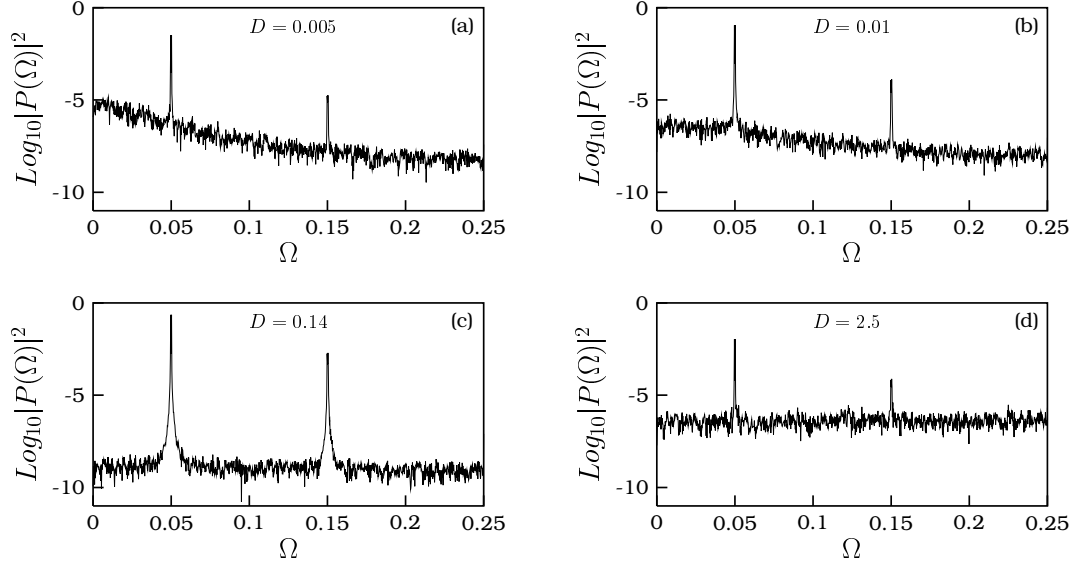


FIG. 8. Power spectral density plot in the presence of square wave for few values of noise intensity D .

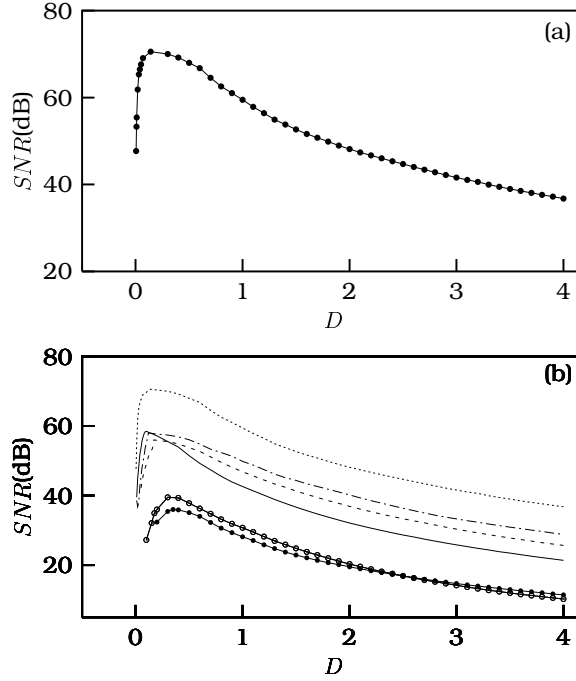


FIG. 9. (a) Signal-to-noise ratio plot for range of values of noise intensity D in the presence of square wave. (b) Signal-to-noise ratio plot for various periodic forces such as sine (continuous curve), square (dotted curve), symmetric saw-tooth ($- \cdot -$ curve), asymmetric saw-tooth (dashed curve), modulus of sine (dots joined by a continuous curve) and rectified sine (circles joined by a continuous curve) used. In all the cases $f = 0.38$ and $\omega = 0.05$.

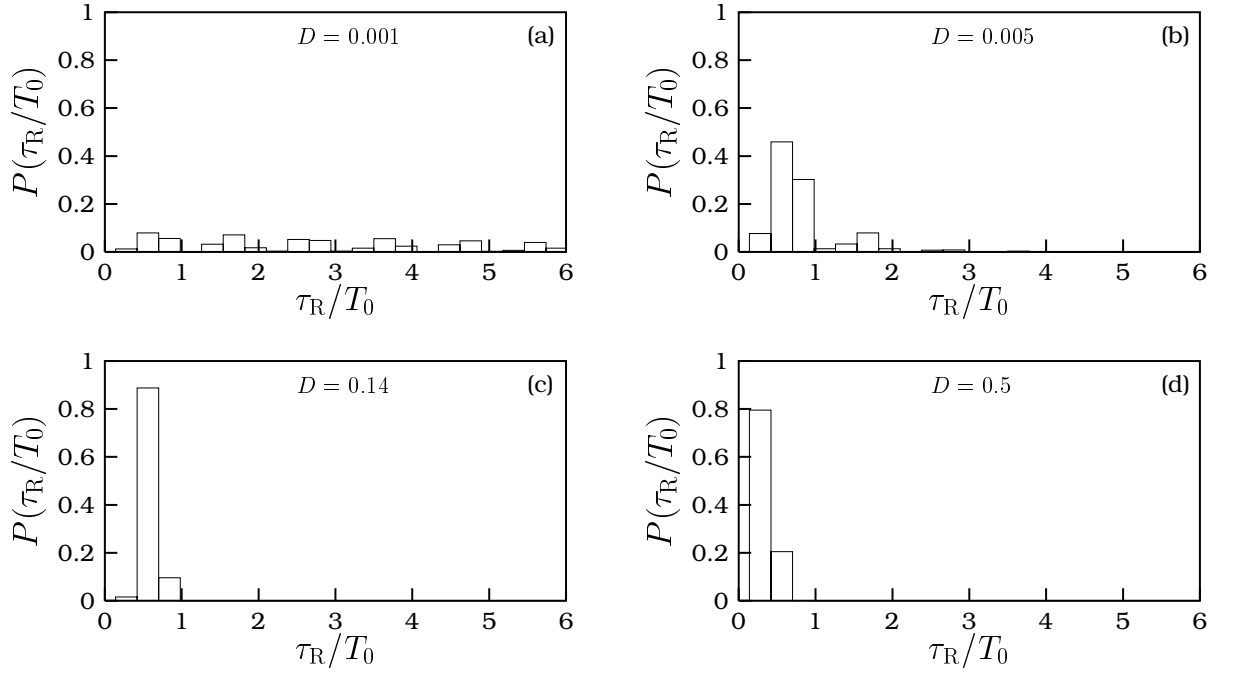


FIG. 10. Normalized residence time distribution for few values of D in the presence of square wave with amplitude $f = 0.38$ and frequency $\omega = 0.05$.

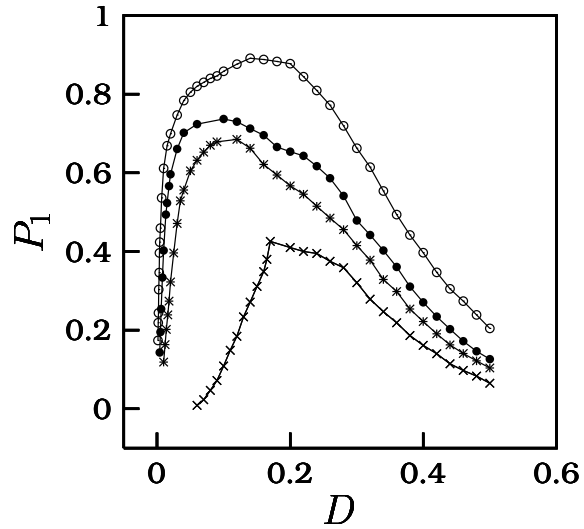


FIG. 11. Height of the peak P_1 in the normalized residence time distribution at $\tau_R = T_0/2$ for square wave (marked by \bullet), sine wave (\circ), symmetric saw-tooth wave ($*$) and asymmetric saw-tooth wave (\times).

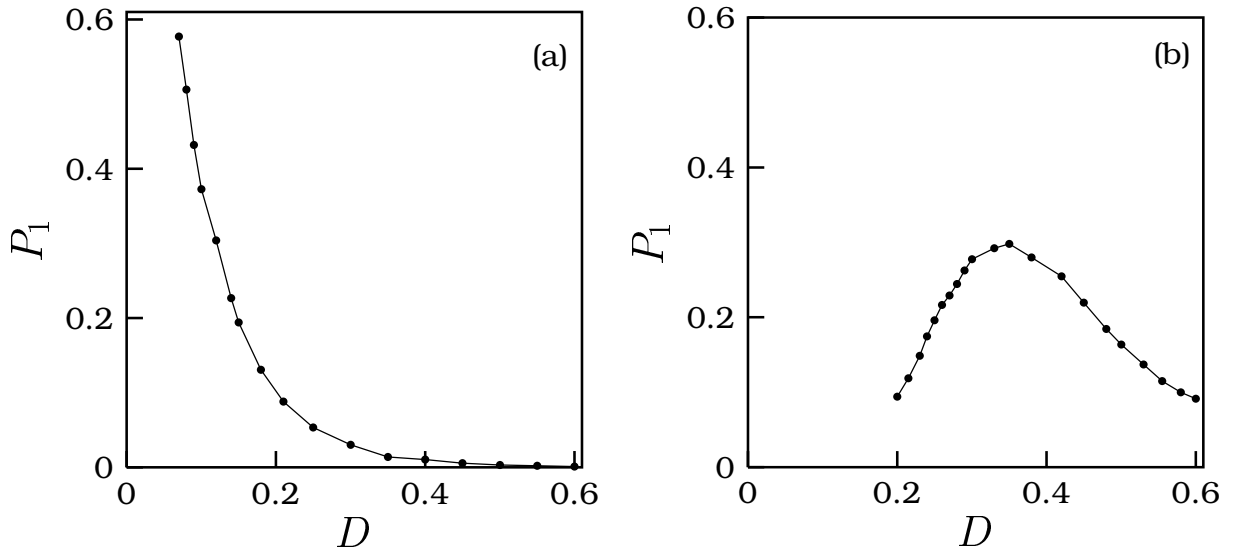


FIG. 12. P_1 versus D for the wells (a) V_{-+} and (b) V_{++} with the applied force as modulus of sine wave.

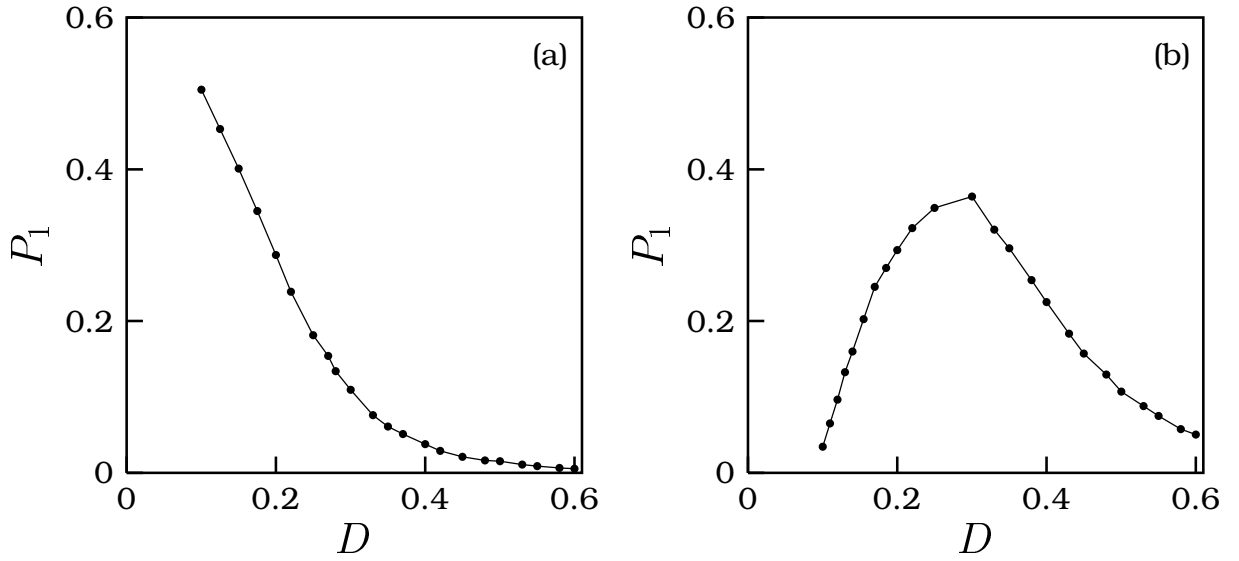


FIG. 13. P_1 versus D for the wells (a) V_{-+} and (b) V_{++} with the applied force as rectified sine wave.